



OPEN ACCESS

EDITED BY

Daniela De Biase,
Sapienza University of Rome, Italy

REVIEWED BY

Javier Carrillo-Campos,
Autonomous University of Chihuahua, Mexico
Alfredo Cabrera-Orefice,
Justus-Liebig University Giessen, Germany

*CORRESPONDENCE

Naoki Takaya
✉ takaya.naoki.ge@u.tsukuba.ac.jp

†PRESENT ADDRESS

Chihiro Kadooka,
Department of Biotechnology and Life
Sciences, Faculty of Biotechnology and Life
Sciences, Sojo University, Kumamoto, Japan

†These authors have contributed equally to
this work

RECEIVED 04 August 2024

ACCEPTED 27 September 2024

PUBLISHED 11 October 2024

CITATION

Kadooka C, Katsuki N, Masuo S, Kojima S,
Amahisa M, Suzuki K, Doi Y, Takeshita N and
Takaya N (2024) Fungal glyceraldehyde
3-phosphate dehydrogenase GpdC maintains
glycolytic mechanism against reactive
nitrogen stress-induced damage.
Front. Microbiol. 15:1475567.
doi: 10.3389/fmicb.2024.1475567

COPYRIGHT

© 2024 Kadooka, Katsuki, Masuo, Kojima,
Amahisa, Suzuki, Doi, Takeshita and Takaya.
This is an open-access article distributed
under the terms of the [Creative Commons
Attribution License \(CC BY\)](https://creativecommons.org/licenses/by/4.0/). The use,
distribution or reproduction in other forums is
permitted, provided the original author(s) and
the copyright owner(s) are credited and that
the original publication in this journal is cited,
in accordance with accepted academic
practice. No use, distribution or reproduction
is permitted which does not comply with
these terms.

Fungal glyceraldehyde 3-phosphate dehydrogenase GpdC maintains glycolytic mechanism against reactive nitrogen stress-induced damage

Chihiro Kadooka^{††}, Nozomi Katsuki[†], Shunsuke Masuo,
Saito Kojima, Madoka Amahisa, Kouta Suzuki, Yuki Doi,
Norio Takeshita and Naoki Takaya*

Faculty of Life and Environmental Sciences, University of Tsukuba, Ibaraki, Japan

Highly reactive nitrogen species (RNS) damage proteins, lipids, and nucleotides, and induce disordered intracellular metabolism. Microorganisms that respond to and defend against RNS include fungal pathogens that invade host tissues. However, the full picture of their mechanisms remains unknown. We identified a novel glyceraldehyde 3-phosphate dehydrogenase (GAPDH) isozyme (GpdC) in the fungus *Aspergillus nidulans*. This isozyme preferred NADP⁺, which was unlike glycolytic GpdA that uses NAD⁺ as a cofactor. Exogenous RNS induced expression of the encoding *gpdC* gene, which when disrupted, decreased intracellular GAPDH activity, mycelial proliferation, and ethanol fermentation under RNS stress. Under these conditions, fungal growth requires glucose instead of non-fermentable carbon sources, and intact pyruvate decarboxylase (*pdca*) and alcohol dehydrogenase (*alcC*) genes indicated that fungal metabolism shifts from respiratory to glycolytic and ethanolic fermentation. These results indicated that GpdC is an alternative GAPDH isozyme that facilitates NADP⁺-dependent glycolysis and energy conservation, which constitutes a fungal mechanism of stress tolerance via metabolic adaptation.

KEYWORDS

nitric oxide, nicotinamide adenine dinucleotide phosphate, ethanol fermentation, glycolysis, *Aspergillus nidulans*

Introduction

Reactive nitrogen species (RNS), especially nitric oxide (NO), play diverse roles in various biological mechanisms including metabolic regulation, signal transduction, and energy conservation (Andrabi et al., 2023). Mammalian NO synthases oxidize arginine to produce NO, and transduce cellular signals (Förstermann and Sessa, 2012; Crane et al., 2010). Plants produce NO from nitrate via nitrate reductase (Yamasaki, 2000; Tiso et al., 2012). Nitric oxide generated from nitrite by nitrite reductases (Zumft et al., 1994; Shoun et al., 1992, Kim et al., 2010) is an intermediate of bacterial and fungal denitrification mechanisms. Bacterial respiratory NO reductases, and fungal cytochrome P450-type NO reductase P450nor participate in these mechanisms by reducing NO to gaseous nitrous oxide (Takaya and Shoun, 2000; Shoun et al., 2012). Fungi and plants assimilate nitrate via nitrite, which is a source of nitrosonium cation (NO⁺) RNS, especially under acidic conditions (Takaya and Shoun, 2000).

Besides playing physiologically important roles, highly reactive RNS are detoxified by organisms to prevent damage to cellular components. Fungal and bacterial

flavohemoglobins oxidize NO to nitrate (Frey et al., 2002; Bonamore and Boffi, 2008; Forrester and Foster, 2012). S-nitrosoglutathione (GSNO) is associated with glutathione and NO metabolism, and GSNO reductase reduces GSNO back to glutathione (Zhou et al., 2016; Liu et al., 2001). Filamentous fungi produce unique tolerating mechanisms in response to RNS. The *Aspergillus nidulans* nitrosothionein-thioredoxin system detoxifies NO (Zhou et al., 2013). A similar function has recently been identified in yeast metallothionein (Yoshikawa et al., 2023). Furthermore, 2,5-diamino-6-(5-phospho-D-ribosylamino)pyrimidin-4(3H)-one is an intermediate of riboflavin synthesis in the yeast *Saccharomyces cerevisiae*, and it scavenges NO (Anam et al., 2020). Amino acid-biosynthesis mechanisms regulated in the presence of RNS govern metabolic adaptation for fungal survival (Amahisa et al., 2024). These and as yet unidentified fungal tolerating mechanisms of RNS are potential targets of antifungal agents because filamentous fungi, especially those in the phylum Ascomycota, which include human pathogens, defend against NO generated by infected hosts (Bogdan, 2001; Martínez-Medina et al., 2019).

Glyceraldehyde 3-phosphate (GAP) dehydrogenase (GAPDH; phosphorylating; E C. 1.2.1.12) catalyzes NAD⁺-dependent redox-coupled phosphorylation of GAP, and it is a key enzyme in glycolytic metabolism (Michels et al., 1996; Weber and Bernhard, 1982). It is also a target of reactive oxygen species (ROS) and RNS, the latter of which post-translationally modifies its thiol moiety at catalytic cysteine to disulfide, S-sulfonyl, S-sulfhydration, S-glutathione and S-nitrosation (Hara et al., 2005; Mustafa et al., 2009; Grant et al., 1999; Tsuchiya et al., 2018). These modifications inactivate GAPDH and regulate signal transduction, transcriptional regulation, and direct the cell fate to either apoptosis or programmed-cell death according to cellular redox status (Hara et al., 2006; Tossounian et al., 2020). Most bacterial and mammalian genomes encode only GAPDH, whereas fungal and plant genomes encode many GAPDH isozymes. The model plant *Arabidopsis thaliana* has seven genes that encode cytosolic NAD⁺-dependent GAPDH and chloroplast NADP⁺-dependent GAPDH (Martin and Cerff, 1986; Hildebrandt et al., 2015). Fungi produce glycolytic NAD⁺-dependent GAPDH encoded by *gpdA*, according to the nomenclature of the genus *Aspergillus* (Flipphi et al., 2009), under glycolysis. Functions other than glycolysis and post-translational modification of the fungal GpdA remain uncharacterized. Another GAPDH ortholog *gpdB* is distributed in most, but not all *Aspergillus* species. The *Aspergillus oryzae* GAPDH isozyme encoded by *gpdB* is resistant to a GAPDH inhibitor of heptelidic acid (Shinohara et al., 2019). The gene is synonymous with *hepG* that resides in the *hep* gene cluster for biosynthesizing the secondary metabolite heptelidic acid, suggesting its function in fungi that produce this antibiotic. The *gpdC* genes are more distantly related to *gpdA* and *gpdB*, and are predicted in *Aspergillus* genomes (Flipphi et al., 2009), but their physiological functions remain unclear.

This study identified a novel *A. nidulans* mechanism of RNS tolerance mediated by the GAPDH ortholog *gpdC*, the transcriptional level of which was increased by exposure to RNS. Analyzing its gene disruptant indicated that GpdC activity is important for glycolysis, ethanol fermentation mechanisms, and cell growth under RNS stress. The enzymatic reaction of GpdC prefers NADP⁺, which is distinct from GpdA that uses NAD⁺ as a cofactor, indicating that the NADP⁺-dependent GAPDH activity of GpdC tolerates RNS stress.

Materials and methods

Strains and growth conditions

We analyzed various strains of *Aspergillus nidulans* (Supplementary Table S1). Mitochondria in the SRS29 (Suelmann and Fischer, 2000) strain were assessed using fluorescence microscopy. *Aspergillus nidulans* strains were cultivated in Minimal Medium (MM; 10 g/L glucose, 6 g/L NaNO₃ or 1.84 g/L ammonium tartrate, 0.52 g/L KCl, 0.52 g/L MgSO₄·7H₂O, 1.52 g/L KH₂PO₄, 1 mL/L Hutner's trace element solution, pH 6.5). The pH of the medium was adjusted using 0.1 M NaOH. We added 0.05 mg/L pyridoxine, 1.22 g/L uracil +1.21 g/L uridine to the medium to cultivate the TN02A3 strain (Nayak et al., 2006). Sodium nitrite was added to sterilized medium, then the pH was adjusted to 5.5. Plasmids were manipulated and proteins were generated in *Escherichia coli* DH5α and BL21 (DE3) strains cultured in LB medium (5 g/L yeast extract, 10 g/L tryptone, 10 g/L NaCl).

Construction of *Aspergillus nidulans* gene disruptants

The *gpdC* (Gene ID, AN2583), *pdcA* (AN4888), *alcC* (AN2286), and *dldA* (AN9066; *S. cerevisiae* *DLD1* ortholog) genes were replaced with the *pyrG* gene in *A. nidulans* TN02A3. We amplified DNA fragments encoding the 5'- and 3'-regions of the *gpdC*, *pdcA*, *alcC*, and *dldA* genes by PCR using the primer sets xxxX-FC/xxxX-R1, and xxxX-F3/xxxX-RC ("xxxX" represent gene names; Supplementary Table S2). Fragments of *pyrG* DNA were amplified by PCR using the primers *pyrG*-F and *pyrG*-R. The PCR template was genomic DNA of *A. nidulans* FGSC A4. Amplified fragments were fused by PCR using the primers xxxX-F1 and xxxX-R3, and transformed into *A. nidulans* TN02A3. Transformants were grown on MM agar. Gene disruption was confirmed by PCR using the primers xxxX-FC and xxxX-RC. Resulting disruptants were designated GpdCΔ, PdcAΔ, AlcCΔ, and DldAΔ (Supplementary Figure S1). The NPC1 strain constructed by introducing a *pyrG* gene fragment at the chromosomal *pyrG89* loci of the TN02A3 strain was the control (Supplementary Table S1).

Introduction of *gpdC* to the GpdCΔ strain

We generated DNA fragments encoding the 5'-regions of *gpdC*, ORF of *gpdC*, and the 3'-region of *pyrG* by PCR using the primer sets: *gpdC*-FC/*gpdC*comp-R1, *gpdC*comp-F2/*gpdC*comp-R2, and *gpdC*comp-F4/*gpdC*comp-RC, respectively (Supplementary Table S2). Genomic DNA of *A. nidulans* FGSC A4 was the template. The *ptrA* gene was a selection marker and corresponding DNA fragments were amplified using the primers *gpdC*comp-F3/*gpdC*comp-R3, and pPTRI (Kubodera et al., 2002). Resultant amplicons were fused by PCR using the primers *gpdC*-F1 and *gpdC*comp-R4 (Supplementary Table S2), and transformed into the GpdCΔ strain. Transformants were cultivated on MM agar containing 0.1 μg/mL pyrithiamine. That *gpdC* was transduced into the target locus to generate the GpdCΔ+*gpdC* strain was confirmed by PCR using the primers *gpdC*-FC and *gpdC*comp-RC (Supplementary Figure S2).

Preparation of recombinant GpdA and GpdC

Conidia (2×10^7) of the *A. nidulans* FGSC A4 strain were rotary shaken in 100 mL of MM at 60 rpm and 37°C for 14 h. Total RNA was extracted from powdered mycelia frozen in liquid nitrogen using RNeasy Plant Mini kits (Qiagen, Hilden, Germany), and cDNA was synthesized using PrimeScript RT Master Mix (Takara Bio, Shiga, Japan) as described by the manufacturer. Complementary DNA fragments for *gpdA* were generated by PCR using fungal cDNA and pET21a-gpdA-F and pET21a-gpdA-R primers (Supplementary Table S2). Complementary DNA fragments for *gpdC* (synthesized at Eurofins Tokyo, Japan) with optimized codons for *E. coli*, were digested by *Nde* I and *Hind* III, then cloned into pET-21a using Ligation High ver. 2 (Toyobo, Osaka, Japan).

Transformants harboring pET21a-gpdA and pET21a-gpdC were rotary-shaken in 3 mL of LB medium at 180 rpm at 37°C for 14 h, then 1 mL portions were inoculated into 100 mL LB medium, and rotary shaken at 160 rpm at 37°C. When the optical density reached 0.6, 0.5 mM isopropyl- β -D(-)-thiogalacto-pyranoside (IPTG) was added to the medium and incubated for 3 h. Harvested cells were resuspended and ultrasonicated in 10 mL of 20 mM HEPES-NaOH buffer (pH 7.5) containing 0.5 M NaCl and 20 mM imidazole, followed by centrifugation at 8,000 $\times g$ for 30 min. Supernatants were passed through a HisTrap FF crude column (Cytiva, North Logan, UT, United States). Thereafter, recombinant GpdA (rGpdA) and GpdC (rGpdC) were eluted with the same buffer containing 200 mM imidazole, and their homogeneity was confirmed by sodium dodecyl sulfate-polyacrylamide gel electrophoresis (SDS-PAGE).

Measurement of GAPDH activities

We added 3 mM GAP to cuvettes containing rGpdA or rGpdC (10 μ g each) in 90 μ L of 1 mM NAD⁺, 10 mM potassium phosphate, 30 mM sodium pyrophosphate (pH 8.4), then changes in absorbance at 340 nm were monitored at 25°C for 2 min using a U-3900 spectrophotometer (Hitachi, Tokyo, Japan). The K_m and k_{cat} values were determined by using 0.01–1 mM NAD⁺, 0.01–10 mM NADP⁺, and 0.015–3 mM GAP. We incubated rGpdA and rGpdC (10 μ g each) dissolved in 20 mM HEPES-NaOH buffer (pH 7.5) containing 150 mM NaCl with NOC-5 and GSNO (Dojindo, Kumamoto, Japan) (0–1 mM each) at 25°C for 1 h, then we analyzed the susceptibility of GAPDH to NO donors.

Quantitative real-time PCR

Aspergillus nidulans FGSC A4 conidia (2×10^7) were inoculated into 100 mL of liquid MM, rotary shaken at 120 rpm and 37°C for 14 h, followed by 10 mM NaNO₂, 3 mM H₂O₂, 50 μ M menadione, 1.5 mM diamide, or 1 mM *tert*-butylhydroperoxide (*t*-BOOH) under the same conditions for 1 h. Mycelial cDNA was prepared as described in Section 1.4, then qRT-PCR proceeded using the THUNDERBIRD® SYBR® qPCR Mix (Toyobo), and the Thermal Cycler Dice Real-Time System MRQ (Takara Bio). Supplementary Table S2 shows the primer sequences.

Measurement of intracellular GAPDH activity

Aspergillus nidulans NPC1 and GpdC Δ conidia (2×10^7) inoculated into 100 mL of liquid MM (pH 5.5) were rotary shaken at 120 rpm and 37°C for 14 h, followed by 120 rpm and 37°C for 0–2 h after adding 10 mM NaNO₂. Powdered mycelia (as described in Section 1.4) were dissolved in 1 mL of 20 mM Tris-HCl containing 150 mM NaCl/0.1 g mycelia, vortex-mixed, then centrifuged for 30 min at 18,800 $\times g$ and 4°C. We assessed GAPDH activity in the supernatant as described (Ralsler et al., 2007) with the following modification. Supernatants (10 μ L) were added to cuvettes containing 1 mM NAD⁺ in 90 μ L of 30 mM sodium pyrophosphate (pH 8.4). The reaction was started by adding 3 mM GAP, then changes in absorbance at 340 nm were monitored at 25°C for 2 min (as described in section 1.5). We then determined the dry weight of lyophilized mycelia.

Determination of cellular GAP and ethanol

Aspergillus nidulans conidia (2×10^7) were cultured and mycelia were prepared as described in section 1.7. Ground mycelial powder (0.1 g) dissolved in 1 mL of 30 mM pyrophosphate buffer (pH 8.4) was vortex-mixed, and centrifuged for 30 min at 18,800 $\times g$ and 4°C. Intracellular GAP was quantified in supernatants as described by Garrigues et al. (1997) and modified as follows. Recombinant GpdA (50 μ g) was added to cuvettes containing 100 μ L of supernatants. Reactions were started by adding 1 mM NAD⁺, and changes in absorbance at 340 nm were monitored at 25°C for 5 min. Ethanol in culture media was quantified using F-kit ethanol (J.K. International, Tokyo, Japan) as described by the manufacturer.

Biotin-switch assays

Recombinant GpdA and GpdC were incubated with 0–0.2 M GSNO at 25°C for 1 h, precipitated using an excess of acetone to remove GSNO, then resuspended in 100 μ L of 20 mM HEPES-NaOH buffer (pH 7.5) containing 150 mM NaCl. Nitrosothiols were modified as described (Li and Kast, 2017) with the following modifications. Suspensions were mixed with equal volumes of 10 mg/mL *N*-ethylmaleimide, incubated at 37°C for 1 h, then proteins were precipitated using acetone. The precipitates were suspended in 100 μ L of 20 mM HEPES-NaOH (pH 7.5) containing 150 mM NaCl, 1 mM biotin-HPDP solution (Dojindo) and 1 mM ascorbic acid, then incubated at 25°C for 1 h. Proteins were resolved by non-reducing SDS-PAGE, then *S*-nitrosothiol detected using horse radish peroxidase-conjugated streptavidin was analyzed by immunoblotting (Cosmo Bio, Tokyo, Japan).

Phylogenetic analysis

Amino acid sequences of fungal GAPDH isozymes were downloaded from the Fungal and Oomycete genomics resource (FungiDB) database (<https://fungidb.org/fungidb/app/>). We analyzed their phylogenies using Molecular Evolutionary Genetics Analysis (MEGA) version 11.0.10 (Tamura et al., 2021).

and the neighbor-joining method with complete gap deletion. Numbers and branches indicate values calculated from 1,000 bootstrap resampling replicates. The amino acid sequence of human GAPDH was obtained from the National Center for Biotechnology, and aligned with the fungal GAPDH using CLUSTALW version 2.1 (Larkin et al., 2007).

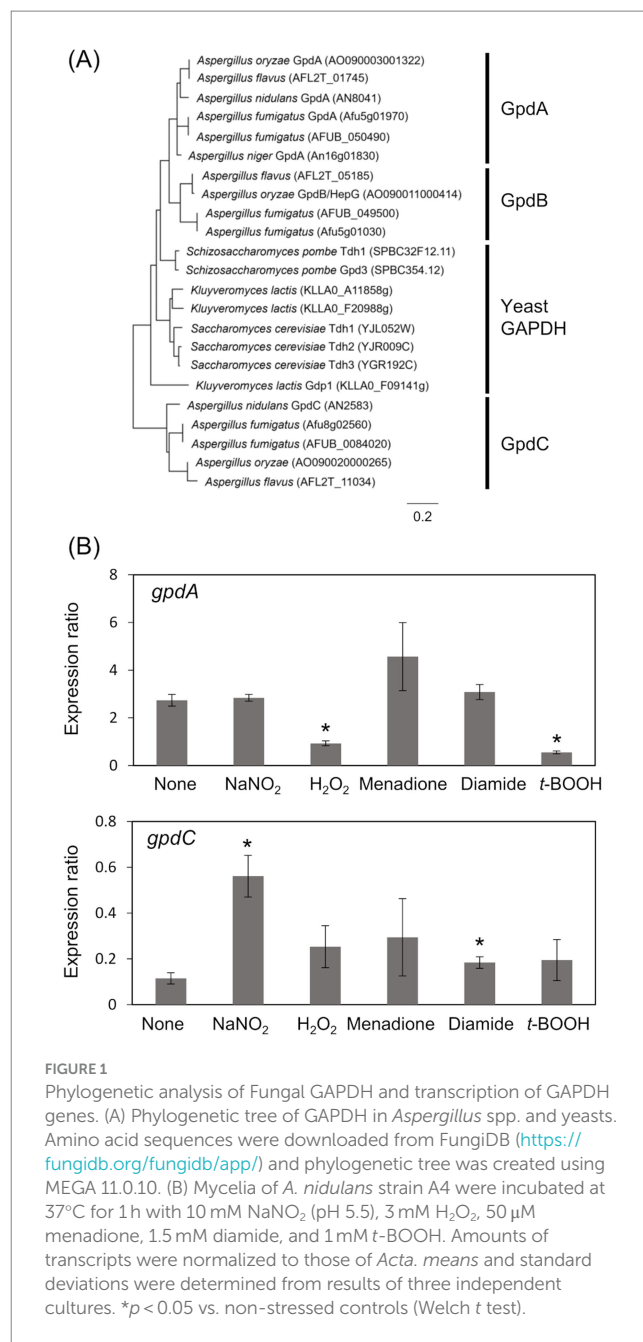
Results

Identification of RNS-inducible *gpdC*

The *A. nidulans* genome consists of *gpdA* (Gene ID, AN8041) that encodes ubiquitous glycolytic GAPDH, and *gpdC* (AN2583) with unknown physiological function. The amino acid sequence identity between GpdA and predicted GpdC proteins was 47.0%. A phylogenetic analysis identified GpdA, B, and C isozymes in all *Aspergillus* species except *A. nidulans*, which lacks a gene encoding GpdB (Figure 1A). Here, we investigated the role of *A. nidulans* GpdC in nitrosative and oxidative stress responses because our transcriptome analysis suggested that *gpdC* expression is upregulated upon exposure to RNS (Amahisa et al., 2024). Transcripts of *gpdC* in *A. nidulans* mycelia were quantified by PCR after exposure to acidified nitrite (1 mM NaNO₂, pH 5.5), H₂O₂, menadione, diamide, and *t*-BOOH as ROS donors for 1 h. We verified that acidified nitrite equilibrated with nitrosonium cations (NO⁺), imposes RNS stress on *A. nidulans* (Zhou et al., 2012). These results indicated that the fungus accumulated 4.9- and 1.6-fold more *gpdC* transcripts after exposure to acidified nitrite and diamide, respectively (Figure 1B). None of the other reagents altered the quantity of intracellular *gpdC* transcripts, whereas that of *gpdA* transcripts was decreased 0.34- and 0.20-fold by H₂O₂ and *t*-BOOH, respectively, but not by acidified nitrite. These results indicated that RNS stress induced *gpdC* expression.

GpdC is a novel fungal NADP⁺- and NAD⁺-dependent GAPDH

Recombinant GpdA (rGpdA) and GpdC (rGpdC) were generated in *E. coli*. Purified proteins migrated as single bands on SDS-PAGE, indicating their homogeneity (Figure 2A). The specific activities of rGpdC on GAP-dependent NAD⁺ and NADP⁺ reduction were 4.1 ± 1.6 and 12 ± 2 μmol min⁻¹ mg⁻¹, respectively. The activities of rGpdA on GAP-dependent NAD⁺ and NADP⁺ reduction were 110 ± 10 and <0.01 μmol min⁻¹ mg⁻¹, indicating that rGpdC and rGpdA oxidize GAP by using NADP⁺ and NAD⁺, and NAD⁺, respectively, as electron acceptors. Steady-state kinetics for the GAP-dependent NAD⁺- and NADP⁺-reduction were analyzed. The apparent Michaelis–Menten (*K_m*) constant of the GpdC reaction for GAP was 290 ± 20 μM, which was similar to that of GpdA (Table 1). The *K_m* value for NAD⁺ was 420 ± 20 μM and comparable to that of rGpdA (410 ± 90 μM). These values were higher than that of NADP⁺ reduction by rGpdC (47 ± 2 μM), indicating that GpdC preferentially uses NADP⁺ over NAD⁺. These results indicated that GpdC is a novel NADP⁺- and NAD⁺-dependent GAPDH. The preference for NADP⁺ over NAD⁺ distinguished GpdC from GpdA, which has very low levels of NADP⁺-dependent GAPDH activity.



The enzymatic activity of mammalian GAPDH is susceptible to oxidative stress due to a ROS-labile catalytic thiol residue (Hara et al., 2006; Sirover, 2014) that reacts with the nitrosating reagent GSNO to generate S-nitrosothiol (Broniowska and Hogg, 2010). Amino acid sequence alignment showed that this thiol residue is conserved in GpdC (Supplementary Figure S4). We investigated the effects of NOC-5 (NO donor) and GSNO on the activities of the fungal GAPDH. After incubation at 25°C for 1 h, NOC-5 concentration-dependently decreased the activity of rGpdA and rGpdC (Figure 2B). At 0.2 mM, NOC-5 impaired the activity of rGpdA more than rGpdC, indicating that rGpdC is more resistant to NO. Adding GSNO also decreased GAPDH activity, but that of rGpdC was more susceptible. Biotin-switch methods visualized S-nitrosothiol of GSNO-treated rGpdA and rGpdC on blots, and this was elevated by increasing the

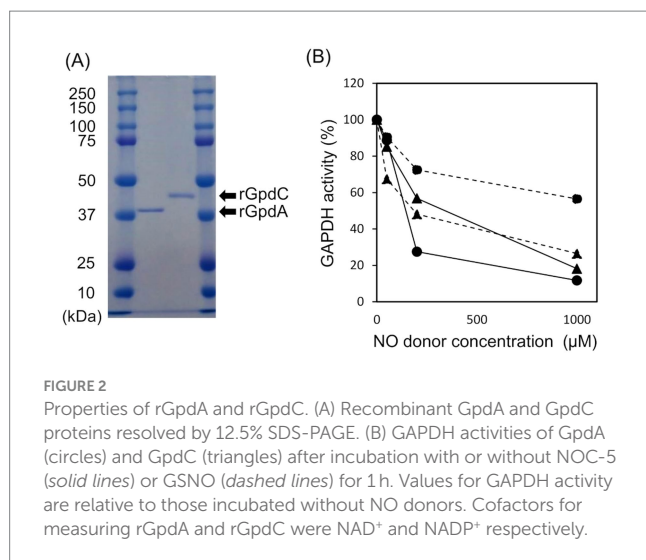


TABLE 1 Apparent kinetic parameters of rGpdA and rGpdC reactions.

Enzyme	Substrate	K_m^{app} (μM)	k_{cat}^{app} (min^{-1})	k_{cat}^{app}/K_m^{app} ($\text{min}^{-1} \mu\text{M}^{-1}$)
GpdA	GAP	410 \pm 90	3,300 \pm 200	7.9 \pm 2.4
	NAD ⁺	180 \pm 30	5,100 \pm 200	28 \pm 7
	NADP ⁺	NA	NA	NA
GpdC	GAP	290 \pm 20	160 \pm 20	0.55 \pm 0.02
	NAD ⁺	420 \pm 20	240 \pm 20	0.56 \pm 0.02
	NADP ⁺	47 \pm 2	530 \pm 30	11 \pm 1

Initial velocity of NADH and NADPH generation was measured in 30 mM sodium pyrophosphate and 10 mM potassium phosphate (pH 8.4) at 25°C. NA, not analyzed due to enzyme activity below detection limit (0.01 $\mu\text{mol min}^{-1} \text{mg}^{-1}$). Data are shown as means \pm standard deviation ($n = 3$).

GSNO concentration (Supplementary Figure S3). This confirmed that GSNO modified the thiol residues of rGpdA and rGpdC to S-nitrosothiol and impaired enzyme activity. The multiple alignment of GAPDH isozymes found five unique Cys residues in GpdC that were not found in human GAPDH and GpdA (Supplementary Figure S4). We consider that this finding complements the higher levels of nitrosation in GpdC (Supplementary Figure S3) because these residues provided extra thiol targets of the nitrosating reagents in GpdC.

GpdC activity is required for growth under RNS stress

Intracellular GAPDH activity produced by the NPC1 (control *gpdC*⁺) strain and GpdC Δ that lacks intact *gpdC* (Supplementary Figure S1) were determined. Mycelia of the strains produced similar levels of activity in the absence of RNS stress, indicating that GpdC is not required for cellular GAPDH activity under these conditions (Figure 3A). This agreed with decreased *gpdC* expression in the absence of stress (Figure 2). Exposure to acidified nitrite (pH 5.5) for 2 h obviously decreased GAPDH activity, indicating impairment by RNS probably due to an oxidation-labile

thiolate residue at the catalytic cysteine. This decrease was more prominent in the GpdC Δ strain that generated little GAPDH activity after exposure to acidified nitrite, which was consistent with the finding that this strain accumulated 1.7-fold more GAP than the NPC1 strain (Figure 3B). These results indicated that GpdC maintains cellular GAPDH activity, and that GpdC replaces RNS-sensitive GpdA under RNS stress.

The GpdC Δ strain grew slowly on agar containing acidified nitrite and H₂O₂ (Figure 3C). The growth rate was more rapid for the GpdC Δ , than the NPC1 strain in the presence of the NO donor diethylenetriamine (DETA)/NO adduct (NOC-18). Under these conditions, GpdC Δ produced a reddish brown pigment in the medium, which was not evident in the NPC1 strain (Figure 3D). Introducing *gpdC* into the GpdC Δ strain restored the growth rate of the strain (GpdC Δ + *gpdC*; Figure 3D), indicating that *gpdC* complemented the growth deficiency of the Δ *gpdC* strains. These results indicated that GpdC is a GAPDH isozyme, the activity of which confers *A. nidulans* growth tolerance under RNS stress.

Reactive nitrogen stress promotes increased dependence on glycolytic metabolism

Reactive nitrogen species react with cellular thiols and metal ions, and mostly abrogate the respiration mechanisms of eukaryotic (Poderoso et al., 2019) and *A. nidulans* mitochondria (Amahisa et al., 2024; Zhou et al., 2012). These conditions might lead to increased dependence of the fungal growth on the glycolytic system. Figure 4A indicate that the acidified nitrite inhibited NPC1 growth more on agar media containing non-glycolytic glycerol, acetate, and glutamate as the carbon source compared with glucose. This suggested the importance of the glycolytic mechanism for fungal growth under RNS stress. The gene disruptants PdcA Δ (without *pdca* encoding glycolytic pyruvate decarboxylase), AlcC Δ (*alcC*, alcohol dehydrogenase), and DldA Δ (*dldA*, putative lactate dehydrogenase) (Grahl et al., 2011) grew at comparable rates on medium containing glucose in the absence of RNS stress (Figure 5A). Acidified nitrite retarded the growth rates of PdcA Δ and AlcC Δ whereas these rates were comparable between DldA Δ and the control strain. These results indicated that the glycolytic ethanol fermentation mechanism is important for fungal growth under RNS stress.

Mitochondria were visualized using mitochondrial citrate synthase (CitA) fused to green fluorescent protein (GFP). Fluorescence shaped filaments, which are typical of fungal mitochondria under stress-free conditions (Figure 4B) dispersed into dot-like structures upon exposure to acidified nitrite. This dot-like morphology is also similar in fungal mitochondria under oxidative stress (Ruf et al., 2018). These results suggested that the RNS stress causes mitochondrial dysfunction and increased fungal metabolic dependence on glycolysis for proliferation.

GpdC replaces GpdA in the glycolytic ethanol fermentation under RNS stress

We analyzed ethanol fermentation to understand the glycolytic role of GpdC under RNS stress. The NPC1 and GpdC Δ strains accumulated the same amounts of ethanol in culture media without acidified nitrite,

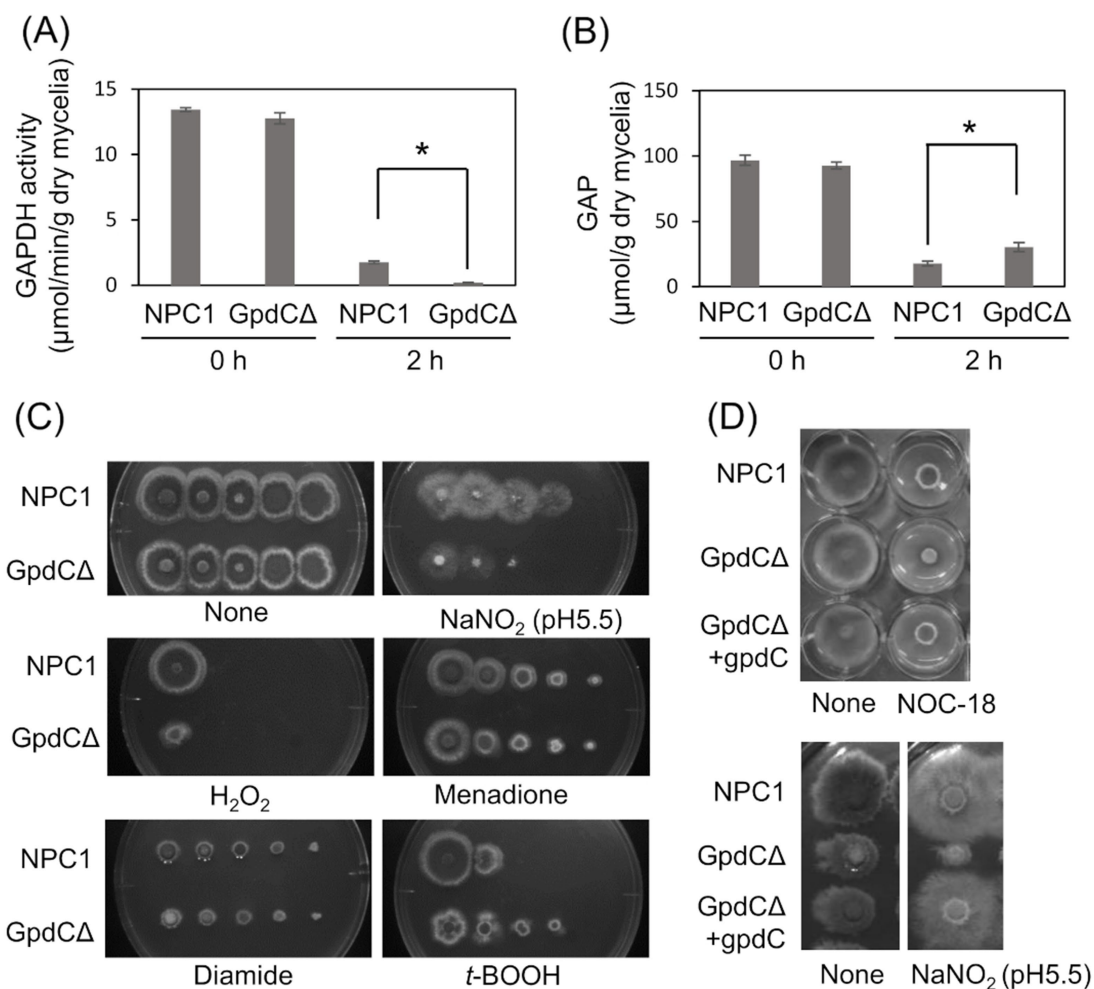


FIGURE 3

GpdC is required for fungal growth under RNS stress. (A) Activities of GAPDH produced by NPC1 and GpdC Δ strains incubated in MM for 14 h, followed by 0 and 2 h with 10 mM NaNO₂. (B) Concentrations of GAP in NPC1 and GpdC Δ strains prepared as shown in panel A. *means* and standard deviations were determined from three independent cultures. * $p < 0.05$ (Welch t tests). (C) Strains NPC1 and GpdC Δ were incubated with MM agar (pH 5.5) with or without 30 mM NaNO₂, 3 mM H₂O₂, 50 μM menadione, 1.5 mM diamide, and 1 mM t -BOOH at 37°C for 3 d. (D) Strains NPC1, GpdC Δ , and GpdC Δ + gpdC were incubated with MM agar (pH 5.5) supplemented with 10 mM NOC-18 and 30 mM NaNO₂ at 37°C for 3 d. Assays including NOC-18 used NaNO₂ as the nitrogen source and pH 6.5 was maintained in MM to avoid NOC-18 instability caused by pH decreases during culture. MM, minimal medium.

whereas PdcA Δ and AlcC Δ accumulated 0.69- and 0.25-fold less ethanol than the NPC1 strain (Figure 5B). In contrast, GpdC Δ produced 0.16-fold more ethanol than the control strain, whereas PdcA Δ and AlcC Δ produced very little under RNS stress. Together with the defective growth under RNS stress (Figure 3), these results indicated that *A. nidulans* GpdC plays a significant role in energy conservation via ethanol fermentation as a mechanism to survive RNS stress.

Figure 6 shows the mechanism of how GpdC renders confers fungal tolerance of RNS stress. The activity of canonical GpdA is largely impaired under RNS stress. *Aspergillus nidulans* induces expression of the *gpdC* gene and maintains intracellular levels of GAPDH activity. Increased tolerance against NO (Figure 2B) agrees with the notion that GpdC replaces GpdA. The NADP⁺-dependent activity of GpdC might contribute to maintain fungal glycolysis because NADPH production is associated with fungal oxidative and RNS stress responses (Yoshikawa et al., 2021). Thus, GpdC functions as an alternative to GpdA under RNS

stress, whereas respiratory/mitochondrial defects increase the dependence of cellular energetic metabolism on a glycolytic mechanism.

Discussion

This study uncovered a novel GAPDH, GpdC, that prefers NADP⁺ for catalysis. Plants and photosynthetic bacteria use NADP⁺-dependent GAPDH, which is involved in photosynthetic carbon fixation and gluconeogenesis, but not in glycolysis (Koksharova et al., 1998). Non-photosynthetic bacteria produce NAD⁺- and NADP⁺-dependent GAPDH to, respectively, facilitate glycolysis and gluconeogenesis (Fillinger et al., 2000). *Kluyveromyces lactis* Gdp1 was the first fungal NADP⁺-dependent GAPDH to be discovered, and it was thought to regenerate NADPH from NADP⁺ produced during xylose assimilation (Verho et al., 2002). The present study is the first to identify a

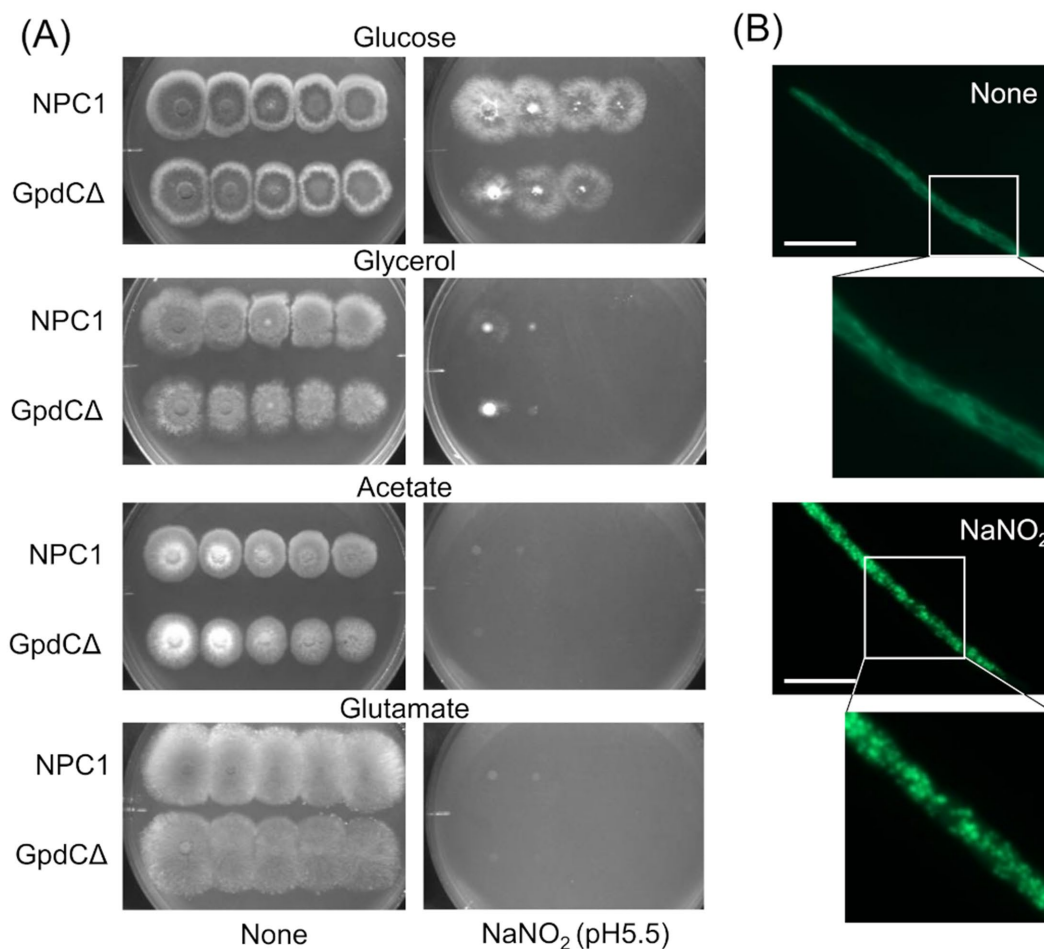


FIGURE 4

Growth of GpdC Δ using carbon sources and morphology of mitochondria under RNS stress. (A) Strains NPC1 and Δ gpdC were incubated on MM agar (pH 5.5) containing 1% glucose, 1% glycerol, 1% sodium acetate, or 1% sodium glutamate with or without 30 mM NaNO₂ at 37°C for 3 d. (B) Mitochondria in strain SRS29 visualized by fluorescence microscopy of GFP. Scale bars, 10 μ m.

glyceraldehyde 3-phosphate dehydrogenase GpdC as an NADP⁺-dependent GAPDH isozyme that is involved in the glycolytic mechanism and the ability of fungal cells to proliferate under RNS stress. This finding expands the diversity of GAPDH functions.

Kluyveromyces lactis Gdp1 is more similar to GpdA than GpdC (54.0% vs. 44.9% amino acid identity). A phylogenetic analysis indicated that it is closely related to GpdA (Figure 1A). A search of a published database showed that although GpdA-like GAPDH is widely distributed in fungi, GpdC-like GAPDH is found only in the fungal genera *Aspergillus*, *Botrytis*, and *Cryptococcus* (Flipphi et al., 2009). These genera include common plant and human pathogens. Considering that organisms develop functional orthologs under specific selection pressures, these fungi have acquired GpdC to survive the life-threatening environment of RNS. Nitric oxide produced by animal and plant NO synthases at sites of infected tissues can generate such an environment.

This study found that, GpdC loses more GAPDH activity than GpdA at lower GSNO concentrations (Figure 2B), indicating that tolerance against this level of RNS does not need GpdC to

substitute the fungal glycolytic function of GpdA under RNS stress. The tolerance of the GpdC mechanism against RNS could be explained by its dependence on NADP⁺ activity. Under oxidative stress, metabolic flux shifts from the glycolytic, to the pentose phosphate pathway in *A. nidulans*, and increases intracellular levels of NADPH (Ralser et al., 2007; Ralser et al., 2009; Talwar et al., 2023) that serves as a cofactor for antioxidant proteins, glutathione reductase (Sato et al., 2009), NO dioxygenase/flavo-hemoglobin, and thioredoxin reductase (Thön et al., 2007; Zhou et al., 2013). Their antioxidant reactions consequently generate NADP⁺. The NADP⁺-dependent GAPDH activity of GpdC enables *A. nidulans* to regenerate NADPH with concomitant glycolytic GAP oxidation, and hence conserves energy under RNS stress.

Mitochondrial dysfunction (Zhou et al., 2012; Amahisa et al., 2024) and disabled utilization of non-fermentable carbon sources by fungi exposed to RNS (Figure 5) evoke RNS stress that alters global cellular metabolism. We found here that RNS decreases the mitochondrial metabolic TCA cycle and amino acid biosynthesis

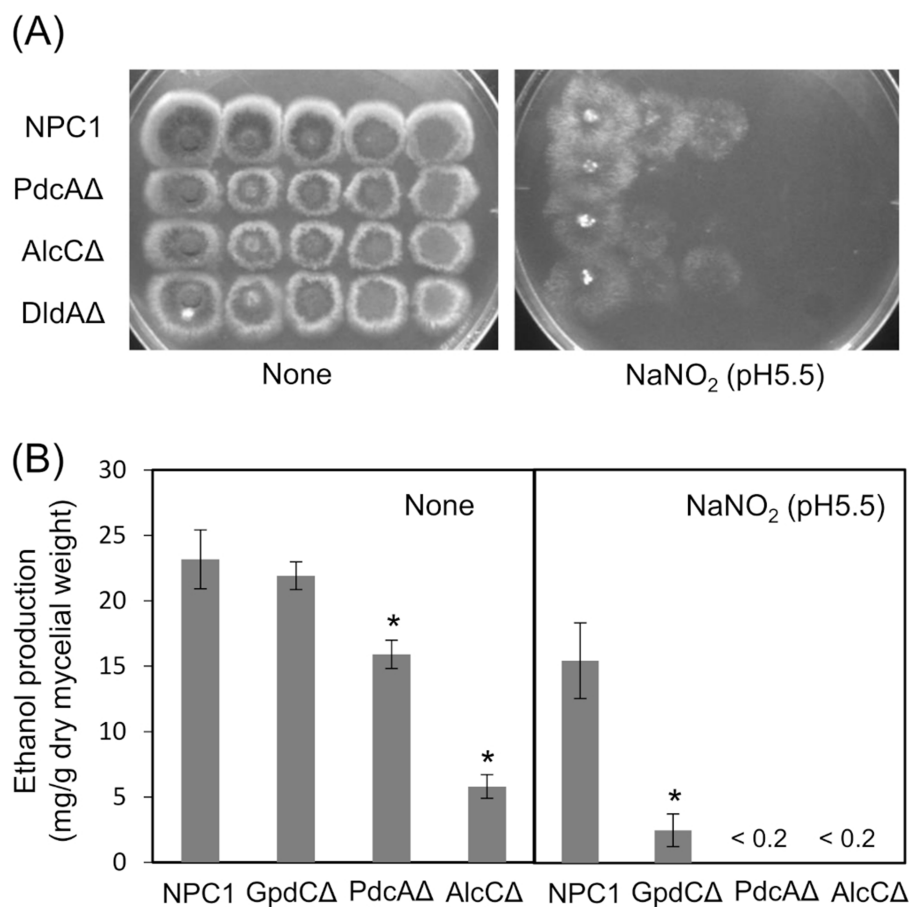


FIGURE 5

Glycolytic mechanism supports fungal growth under RNS stress. (A) Growth of NPC1, PdcAΔ, AlcCΔ and DldAΔ on MM agar (pH 5.5) supplemented with or without 30 mM NaNO₂ at 37°C for 3. (B) Ethanol production by NPC1, GpdCΔ, PdcAΔ and AlcCΔ strains incubated in MM (pH 5.5) for 14 h followed by 12 h with 10 mM NaNO₂. Means and standard deviations were determined from results of three independent cultures. **p* < 0.05 vs. NPC1 (Welch *t* tests).

(Amahisa et al., 2024), which concur with these findings. The fungus responds to RNS, induces the transcription of genes to synthesize amino acids via the master regulator CpcA, which is a counterpart of the yeast Gcn4p operating general amino acid control system, and maintains cellular amino acid synthesis (Amahisa et al., 2024). The finding that GpcC responded to RNS and maintained glycolysis adds another mechanism of metabolic regulation that allows fungi to adapt to RNS. This highlights the importance of metabolic regulation co-operating with RNS detoxification mechanisms mediated by specific proteins and factors (Frey et al., 2002; Liu et al., 2001; Zhou et al., 2013; Yoshikawa et al., 2023; Anam et al., 2020) to fungal responses and resistance to RNS.

Filamentous fungi, especially those in the genus *Aspergillus*, produce many industrially useful fermentation products such as organic acids and enzymes. Efficient production depends on appropriate control of cultures under oxidative and RNS stress. Infective *Aspergillus* pathogens are thought to counteract the RNS produced by NO produced by the host immune system. The discovery of GpdC involved in RNS tolerance might provide new targets to

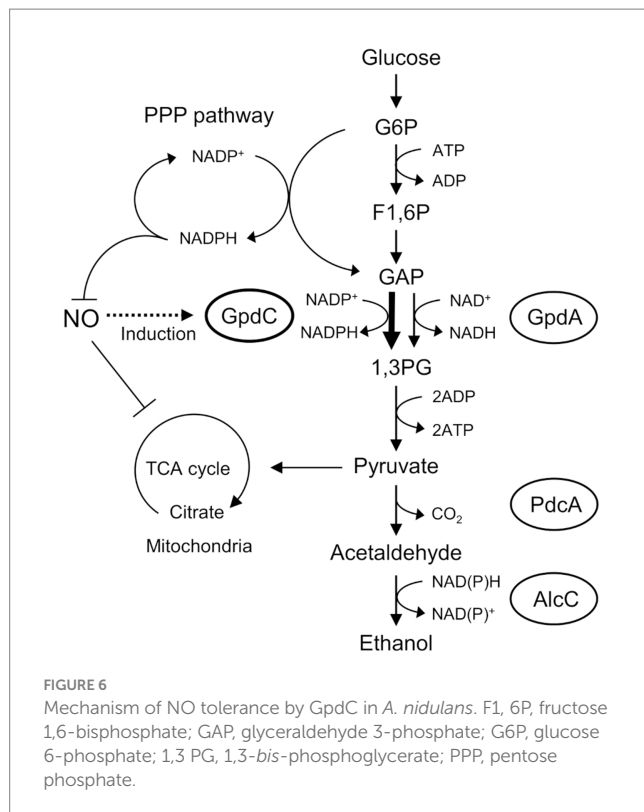
control these fermentation processes and antifungal agents to treat diseases.

Data availability statement

The original contributions presented in the study are included in the article/Supplementary material, further inquiries can be directed to the corresponding author/s.

Author contributions

CK: Funding acquisition, Investigation, Writing – original draft. NK: Investigation, Writing – original draft. SM: Validation, Writing – original draft. SK: Investigation, Writing – original draft. MA: Investigation, Writing – original draft. KS: Investigation, Writing – original draft. YD: Investigation, Writing – original draft. NoT: Supervision, Writing – review & editing. NaT: Conceptualization, Funding acquisition, Writing – original draft, Writing – review & editing.



Funding

The author(s) declare that financial support was received for the research, authorship, and/or publication of this article. This research was funded by JSPS KAKENHI Grant nos. 19H05639 (to NaT) and JP19H05687K (to NaT). C.K. was supported by a Grant-in-Aid for JSPS Research Fellows (20J00169).

Acknowledgments

Strains and plasmids were obtained from the Fungal Genetics Stock Center (Kansas City, MO, United States).

References

- Amahisa, M., Tsukagoshi, M., Kadooka, C., Masuo, S., Takeshita, N., Doi, Y., et al. (2024). The metabolic regulation of amino acid synthesis counteracts reactive nitrogen stress via *Aspergillus nidulans* cross-pathway control. *J. Fungi* 10:58. doi: 10.3390/jof10010058
- Anam, K., Nasuno, R., and Takagi, H. (2020). A novel mechanism for Nitrosative stress tolerance dependent on GTP Cyclohydrolase II activity involved in riboflavin synthesis of yeast. *Sci. Rep.* 10:6015. doi: 10.1038/s41598-020-62890-3
- Andrabi, S. M., Sharma, N. S., Karan, A., Shahriar, S. M. S., Cordon, B., Ma, B., et al. (2023). Nitric oxide: physiological functions, delivery, and biomedical applications. *Adv. Sci. (Weinh)* 10:e2303259. doi: 10.1002/advsc.202303259
- Bogdan, C. (2001). Nitric oxide and the immune response. *Nat. Immunol.* 2, 907–916. doi: 10.1038/ni1001-907
- Bonamore, A., and Boffi, A. (2008). Flavohemoglobin: structure and reactivity. *IUBMB Life* 60, 19–28. doi: 10.1002/iub.9
- Broniowska, K. A., and Hogg, N. (2010). Differential mechanisms of inhibition of glyceraldehyde-3-phosphate dehydrogenase by S-nitrosothiols and NO in cellular and cell-free conditions. *Am. J. Physiol. Heart Circ. Physiol.* 299, H1212–H1219. doi: 10.1152/ajpheart.00472.2010
- Crane, B. R., Sudhamsu, J., and Patel, B. A. (2010). Bacterial nitric oxide synthases. *Annu. Rev. Biochem.* 79, 445–470. doi: 10.1146/annurev-biochem-062608-103436
- Fillinger, S., Boschi-Muller, S., Azza, S., Dervyn, E., Branlant, G., and Aymerich, S. (2000). Two glyceraldehyde-3-phosphate dehydrogenases with opposite physiological roles in a nonphotosynthetic bacterium. *J. Biol. Chem.* 275, 14031–14037. doi: 10.1074/jbc.275.19.14031
- Flippi, M., Sun, J., Robellet, X., Karaffa, L., Fekete, E., Zeng, A. P., et al. (2009). Biodiversity and evolution of primary carbon metabolism in *Aspergillus nidulans* and other *Aspergillus* spp. *Fungal Genet. Biol.* 46, S19–S44. doi: 10.1016/j.fgb.2008.07.018
- Forrester, M. T., and Foster, M. W. (2012). Protection from nitrosative stress: a central role for microbial flavohemoglobin. *Free Radic. Biol. Med.* 52, 1620–1633. doi: 10.1016/j.freeradbiomed.2012.01.028
- Förstermann, U., and Sessa, W. C. (2012). Nitric oxide synthases: regulation and function. *Eur. Heart J.* 33, 829–837. doi: 10.1093/eurheartj/ehr304
- Frey, A. D., Farrés, J., Bollinger, C. J., and Kallio, P. T. (2002). Bacterial hemoglobins and flavohemoglobins for alleviation of nitrosative stress in *Escherichia coli*. *Appl. Environ. Microbiol.* 68, 4835–4840. doi: 10.1128/AEM.68.10.4835-4840.2002

Conflict of interest

The authors declare that the research was conducted in the absence of any commercial or financial relationships that could be construed as a potential conflict of interest.

Publisher's note

All claims expressed in this article are solely those of the authors and do not necessarily represent those of their affiliated organizations, or those of the publisher, the editors and the reviewers. Any product that may be evaluated in this article, or claim that may be made by its manufacturer, is not guaranteed or endorsed by the publisher.

Supplementary material

The Supplementary material for this article can be found online at: <https://www.frontiersin.org/articles/10.3389/fmicb.2024.1475567/full#supplementary-material>

SUPPLEMENTARY FIGURE S1

Construction of *A. nidulans* gene disruptants. (A) Schematic representation of gene disruption. Arrows indicate positions and directions of primers (Supplementary Table S1). (B) Disruption of transformant genes confirmed by PCR.

SUPPLEMENTARY FIGURE S2

Construction of *gpdC* and *gpdC*-complementation strains. (A) Schematic representation of gene disruption. Arrows indicate positions and directions of primers (Supplementary Table S1). (B) Disruption of transformant genes confirmed by PCR.

SUPPLEMENTARY FIGURE S3

Detection of S-nitrosylated GAPDH. Upper panel: Biotin-switch assay of S-nitrosothiol 0, 1, 10, 50, 100, or 200 μ M GSNO to 1 μ g of purified GpdA and GpdC using streptavidin-conjugated horseradish peroxidase. Lower panel: protein detected using Ponceau S.

SUPPLEMENTARY FIGURE S4

Multiple amino acid sequence alignment of GAPDH isozymes. Amino acid residues that were post-translationally modified in mammalian GAPDH are highlighted in light blue (nitrosation/oxidation), yellow (acetylation), and red (phosphorylation). Unique cysteine residues are boxed. Human GAPDH, NP_001276674.1; GpdA, AN8041; GpdC, AN2583.

- Garrigues, C., Loubiere, P., Lindley, N. D., and Coccain-Bousquet, M. (1997). Control of the shift from homolactic acid to mixed-acid fermentation in *Lactococcus lactis*: predominant role of the NADH/NAD⁺ ratio. *J. Bacteriol.* 179, 5282–5287. doi: 10.1128/jb.179.17.5282-5287.1997
- Grahl, N., Puttikamonkul, S., Macdonald, J. M., Gamcsik, M. P., Ngo, L. Y., Hohl, T. M., et al. (2011). In vivo hypoxia and a fungal alcohol dehydrogenase influence the pathogenesis of invasive pulmonary aspergillosis. *PLoS Pathog.* 7:e1002145. doi: 10.1371/journal.ppat.1002145
- Grant, C. M., Quinn, K. A., and Dawes, I. W. (1999). Differential protein S-thiolation of glyceraldehyde-3-phosphate dehydrogenase isoenzymes influences sensitivity to oxidative stress. *Mol. Cell. Biol.* 19, 2650–2656. doi: 10.1128/MCB.19.4.2650
- Hara, M. R., Agrawal, N., Kim, S. F., Cascio, M. B., Fujimuro, M., Ozeki, Y., et al. (2005). S-nitrosylated GAPDH initiates apoptotic cell death by nuclear translocation following Siah1 binding. *Nat. Cell Biol.* 7, 665–674. doi: 10.1038/ncb1268
- Hara, M. R., Cascio, M. B., and Sawa, A. (2006). GAPDH as a sensor of NO stress. *Biochim. Biophys. Acta* 1762, 502–509. doi: 10.1016/j.bbadis.2006.01.012
- Hildebrandt, T., Knuesting, J., Berndt, C., Morgan, B., and Scheibe, R. (2015). Cytosolic thiol switches regulating basic cellular functions: GAPDH as an information hub? *Biol. Chem.* 396, 523–537. doi: 10.1515/hsz-2014-0295
- Kim, S. W., Fushinobu, S., Zhou, S., Wakagi, T., and Shoun, H. (2010). The possible involvement of copper-containing nitrite reductase (NirK) and flavohemoglobin in denitrification by the fungus *Cylindrocarpum tonkinense*. *Biosci. Biotechnol. Biochem.* 74, 1403–1407. doi: 10.1271/bbb.100071
- Koksharova, O., Schubert, M., Shestakov, S., and Cerff, R. (1998). Genetic and biochemical evidence for distinct key functions of two highly divergent GAPDH genes in catabolic and anabolic carbon flow of the cyanobacterium *Synechocystis* sp. PCC 6803. *Plant Mol. Biol.* 36, 183–194. doi: 10.1023/a:1005925732743
- Kubodera, T., Yamashita, N., and Nishimura, A. (2002). Transformation of aspergillus sp. and *Trichoderma reesei* using the pyriothiamine resistance gene (ptrA) of aspergillus oryzae. *Biosci. Biotechnol. Biochem.* 66, 404–406. doi: 10.1271/bbb.66.404
- Larkin, M. A., Blackshields, G., Brown, N. P., Chenna, R., McGettigan, P. A., McWilliam, H., et al. (2007). Clustal W and Clustal X version 2.0. *Bioinformatics* 23, 2947–2948. doi: 10.1093/bioinformatics/btm404
- Li, R., and Kast, J. (2017). Biotin switch assays for quantitation of reversible cysteine oxidation. *Methods Enzymol.* 585, 269–284. doi: 10.1016/bs.mie.2016.10.006
- Liu, L., Hausladen, A., Zeng, M., Que, L., Heitman, J., and Stamler, J. S. (2001). A metabolic enzyme for S-nitrosothiol conserved from bacteria to humans. *Nature* 410, 490–494. doi: 10.1038/35068596
- Martin, W., and Cerff, R. (1986). Prokaryotic features of a nucleus-encoded enzyme. cDNA sequences for chloroplast and cytosolic glyceraldehyde-3-phosphate dehydrogenases from mustard (*Sinapis alba*). *Eur. J. Biochem.* 159, 323–331. doi: 10.1111/j.1432-1033.1986.tb09871.x
- Martínez-Medina, A., Pescador, L., Terrón-Camero, L. C., Pozo, M. J., and Romero-Puertas, M. C. (2019). Nitric oxide in plant-fungal interactions. *J. Exp. Bot.* 70, 4489–4503. doi: 10.1093/jxb/erz289
- Michels, S., Rogalska, E., and Branlant, G. (1996). Phosphate-binding sites in phosphorylating glyceraldehyde-3-phosphate dehydrogenase from *Bacillus stearothermophilus*. *Eur. J. Biochem.* 235, 641–647. doi: 10.1111/j.1432-1033.1996.00641.x
- Mustafa, A. K., Gadalla, M. M., Sen, N., Kim, S., Mu, W., Gazi, S. K., et al. (2009). H2S signals through protein S-sulfhydration. *Sci. Signal.* 2:ra72. doi: 10.1126/scisignal.2000464
- Nayak, T., Szewczyk, E., Oakley, C. E., Osmani, A., Ukil, L., Murray, S. L., et al. (2006). A versatile and efficient gene-targeting system for *Aspergillus nidulans*. *Genetics* 172, 1557–1566. doi: 10.1534/genetics.105.052563
- Poderoso, J. J., Helfenberger, K., and Poderoso, C. (2019). The effect of nitric oxide on mitochondrial respiration. *Nitric Oxide* 88, 61–72. doi: 10.1016/j.niox.2019.04.005
- Ralsler, M., Wamelink, M. M., Kowald, A., Gerisch, B., Heeren, G., Struys, E. A., et al. (2007). Dynamic rerouting of the carbohydrate flux is key to counteracting oxidative stress. *J. Biol.* 6:10. doi: 10.1186/jbiol61
- Ralsler, M., Wamelink, M. M., Latkolik, S., Jansen, E. E., Lehrach, H., and Jakobs, C. (2009). Metabolic reconfiguration precedes transcriptional regulation in the antioxidant response. *Nat. Biotechnol.* 27, 604–605. doi: 10.1038/nbt0709-604
- Ruf, D., Brantl, V., and Wagener, J. (2018). Mitochondrial fragmentation in *Aspergillus fumigatus* as early marker of granulocyte killing activity. *Front. Cell. Infect. Microbiol.* 8:128. doi: 10.3389/fcimb.2018.00128
- Sato, I., Shimizu, M., Hoshino, T., and Takaya, N. (2009). The glutathione system of *Aspergillus nidulans* involves a fungus-specific glutathione S-transferase. *J. Biol. Chem.* 284, 8042–8053. doi: 10.1074/jbc.M80771200
- Shinohara, Y., Nishimura, I., and Koyama, Y. (2019). Identification of a gene cluster for biosynthesis of the sesquiterpene antibiotic, heptelidic acid, in *Aspergillus oryzae*. *Biosci. Biotechnol. Biochem.* 83, 1506–1513. doi: 10.1080/09168451.2018.1549934
- Shoun, H., Fushinobu, S., Jiang, L., Kim, S. W., and Wakagi, T. (2012). Fungal denitrification and nitric oxide reductase cytochrome P450nor. *Philos. Trans. R. Soc. Lond. Ser. B Biol. Sci.* 367, 1186–1194. doi: 10.1098/rstb.2011.0335
- Shoun, H., Kim, D. H., Uchiyama, H., and Sugiyama, J. (1992). Denitrification by fungi. *FEMS Microbiol. Lett.* 94, 277–281. doi: 10.1016/0378-1097(92)90643-3
- Sirover, M. A. (2014). Structural analysis of glyceraldehyde-3-phosphate dehydrogenase functional diversity. *Int. J. Biochem. Cell Biol.* 57, 20–26. doi: 10.1016/j.biocel.2014.09.026
- Suelmann, R., and Fischer, R. (2000). Mitochondrial movement and morphology depend on an intact actin cytoskeleton in *Aspergillus nidulans*. *Cell Motil. Cytoskeleton* 45, 42–50. doi: 10.1002/(SICI)1097-0169(200001)45:1<42::AID-CM4>3.0.CO;2-C
- Takaya, N., and Shoun, H. (2000). Nitric oxide reduction, the last step in denitrification by *Fusarium oxysporum*, is obligatorily mediated by cytochrome P450nor. *Mol. Gen. Genet.* 263, 342–348. doi: 10.1007/s004380051177
- Talwar, D., Miller, C. G., Grossmann, J., Szyrwił, L., Schwewe, T., Demichev, V., et al. (2023). The GAPDH redox switch safeguards reductive capacity and enables survival of stressed tumour cells. *Nat. Metab.* 5, 660–676. doi: 10.1038/s42255-023-00781-3
- Tamura, K., Stecher, G., and Kumar, S. (2021). MEGA11: molecular evolutionary genetics analysis version 11. *Mol. Biol. Evol.* 38, 3022–3027. doi: 10.1093/molbev/msab120
- Thön, M., Al-Abdallah, Q., Hortschansky, P., and Brakhage, A. A. (2007). The thioredoxin system of the filamentous fungus *Aspergillus nidulans*: impact on development and oxidative stress response. *J. Biol. Chem.* 282, 27259–27269. doi: 10.1074/jbc.M704298200
- Tiso, M., Tejero, J., Kenney, C., Frizzell, S., and Gladwin, M. T. (2012). Nitrite reductase activity of nonsymbiotic hemoglobins from *Arabidopsis thaliana*. *Biochemistry* 51, 5285–5292. doi: 10.1021/bi300570v
- Tossounian, M. A., Zhang, B., and Gout, I. (2020). The writers, readers, and erasers in redox regulation of GAPDH. *Antioxidants (Basel)* 9:1288. doi: 10.3390/antiox9121288
- Tsuchiya, Y., Zhyvoloup, A., Baković, J., Thomas, N., Yu, B. Y. K., Das, S., et al. (2018). Protein CoAlation and antioxidant function of coenzyme a in prokaryotic cells. *Biochem. J.* 475, 1909–1937. doi: 10.1042/BCJ20180043
- Verho, R., Richard, P., Jonson, P. H., Sundqvist, L., Londesborough, J., and Penttilä, M. (2002). Identification of the first fungal NADP-GAPDH from *Kluyveromyces lactis*. *Biochemistry* 41, 13833–13838. doi: 10.1021/bi0265325
- Weber, J. P., and Bernhard, S. A. (1982). Transfer of 1,3-diphosphoglycerate between glyceraldehyde-3-phosphate dehydrogenase and 3-phosphoglycerate kinase via an enzyme-substrate-enzyme complex. *Biochemistry* 21, 4189–4194. doi: 10.1021/bi00260a042
- Yamasaki, H. (2000). Nitrite-dependent nitric oxide production pathway: implications for involvement of active nitrogen species in photoinhibition in vivo. *Philos. Trans. R. Soc. Lond. Ser. B Biol. Sci.* 355, 1477–1488. doi: 10.1098/rstb.2000.0708
- Yoshikawa, Y., Nasuno, R., and Takagi, H. (2021). An NADPH-independent mechanism enhances oxidative and nitrosative stress tolerance in yeast cells lacking glucose-6-phosphate dehydrogenase activity. *Yeast* 38, 414–423. doi: 10.1002/yea.3558
- Yoshikawa, Y., Nasuno, R., Takaya, N., and Takagi, H. (2023). Metallothionein Cup1 attenuates nitrosative stress in the yeast *Saccharomyces cerevisiae*. *Microb. Cell* 10, 170–177. doi: 10.15698/mic2023.08.802
- Zhou, S., Narukami, T., Masuo, S., Shimizu, M., Fujita, T., Doi, Y., et al. (2013). NO-inducible nitrosothionein mediates NO removal in tandem with thioredoxin. *Nat. Chem. Biol.* 9:657–663. doi: 10.1038/nchembio.1316
- Zhou, S., Narukami, T., Nameki, M., Ozawa, T., Kamimura, Y., Hoshino, T., et al. (2012). Heme-biosynthetic porphobilinogen deaminase protects *Aspergillus nidulans* from nitrosative stress. *Appl. Environ. Microbiol.* 78, 103–109. doi: 10.1128/AEM.06195-11
- Zhou, Y., Zhou, S., Yu, H., Li, J., Xia, Y., Li, B., et al. (2016). Cloning and characterization of filamentous fungal S-Nitrosoglutathione reductase from *Aspergillus nidulans*. *J. Microbiol. Biotechnol.* 26, 928–937. doi: 10.4014/jmb.1512.12009
- Zumft, W. G., Braun, C., and Cuypers, H. (1994). Nitric oxide reductase from *Pseudomonas butzeri*. Primary structure and gene organization of a novel bacterial cytochrome bc complex. *Eur. J. Biochem.* 219, 481–490. doi: 10.1111/j.1432-1033.1994.tb19962.x